to the thermal expansion almost entirely by virtue of the effect of the vacancies on the interionic potential. The additional sites created at the surface do not make a significant contribution (less than 1%) to the expansion of the crystal, as Fischmeister has noted.

The available expansion data for NaCl are just barely accurate enough to provide basis for the conclusions here drawn. It should be kept in mind that the contribution of the defects is a *third-order* effect in the measured variable. Additional careful expansion measurements in the high-temperature range, both for NaCl and for other alkali halides, with simultaneous measurement of the high-temperature electrical conductivity, would be very desirable.

PHYSICAL REVIEW VOLUME 125, NUMBER 1 JANUARY 1, 1962

Theory of Field Emission from Semiconductors

ROBERT STRATTON
Central Research Laboratories, Texas Instruments Incorporated, Dallas, Texas
(Received July 3, 1961)

The field emission current density j_c, originating from the conduction band, is derived for an arbitrary degeneracy (i.e., Fermi energy) at the surface. The theory allows for a difference between the effective and free electron masses; detailed results being worked out for spherical energy surfaces. Simple formulas for j_c are presented which involve correction factors that are slowly varying functions of the temperature, field F, and Fermi energy, and have been computed numerically; j_c is approximately proportional to the emission probability of an electron either at the Fermi level or at the bottom of the conduction band for positive or negative Fermi energies, respectively. Strong deviations from linearity, of a $\ln j_c$ versus $(1/F)$ plot, require that the Fermi energy at the surface depend markedly on F. The emission current for the intermediate, or T-F, range is also considered. The field emission current density j_v originating from the valence band is also discussed. As an example, numerical results are given for germanium. For this case, j_v exceeds j_c at room temperature, except when the surface is strongly degenerate n type. The theory is qualitatively consistent with Allen's experimental results for a clean germanium surface.

I. INTRODUCTION

IF a sufficiently intense electric field is applied normal to the surface of a metal or semiconductor, electrons will be emitted, through the surface potential barrier, by the quantum mechanical tunnelling effect. Since the fields required for a measurable current emission are in the range 10^7 to 10^8 v/cm, the experimental arrangement usually consists of a fine needle emitter (radius of curvature of the tip about 10^{-4} cm) placed inside an evacuated chamber, partly lined with a conducting film which collects the electrons. If the surface of the collector, or anode, is also treated with a fluorescent material, characteristic patterns are observed from nearly clean single crystal emitters (electron field emission microscope[1]).

The theory of field emission from metals was first derived by Fowler and Nordheim[2] in 1928, who showed that if the temperature is not too high, most of the emitted electrons originate from a small energy interval around the Fermi level of the metal. At the other extreme, high temperatures and low fields, electron emission over the potential barrier, rather than through it, predominates, i.e., thermionic emission. There is also an intermediate range of fields and temperatures where the electrons tunnel through the barrier but come mainly from energy levels well above the Fermi level in the metal.[3] This process has been called T-F emission by Dolan and Dyke.[4] Experimental and theoretical progress in field emission from metals has recently been reviewed by Good and Müller.[5]

When the theory of field emission from semiconductors was considered by the present author in 1955,[6] there had only been preliminary experimental observations of this effect, using[7] Cs_3Sb and the photoconductors CdS and CdSe.[8] Since then there have been experimental studies of field emission from CdS,[9] CdSe,[9] W_2C,[10–12] Mo_2C,[11] SiC,[13] Al_2O_3,[14] SiO_2,[14] ZnS,[15] Te,[16]

[1] E. W. Müller, Z. Physik **106**, 541 (1937).
[2] R. H. Fowler and L. Nordheim, Proc. Roy. Soc. (London) A119, 173 (1928).
[3] E. Guth and C. J. Mullin, Phys. Rev. **61**, 339 (1942).
[4] W. W. Dolan and W. P. Dyke, Phys. Rev. **95**, 327 (1954).
[5] R. H. Good and E. W. Müller, *Handbuch der Physik*, edited by S. Flügge (Springer-Verlag, Berlin, 1956), Vol. XXI, p. 176.
[6] R. Stratton, Proc. Phys. Soc. (London) **B68**, 746 (1955). (This paper will be referred to as I; equations from it will be preceded by I.) At the time this paper was written the author was unaware of an earlier publication by N. Morgulis, J. Tech. Phys. (U.S.S.R.) **17**, 983 (1947) on field emission from semiconductors. Morgulis derived the effect of weak field penetration (i.e., assuming classical statistics) on electron emission from the conduction band and also gave an approximate estimate for emission from the valence band which, however, differs from our result in Sec. 6.
[7] B. G. Brezhnev. J. Exptl. Theoret. Phys. **17**, 108 (1947).
[8] L. Apker and E. Taft. Phys. Rev. **88**, 1037 (1952).
[9] A. I. Klimin. J. Tech. Phys. (U.S.S.R.) **27**, 719 (1957) [translation: Soviet Phys. (Tech. Phys.) **2**, 649 (1957)].
[10] I. I. Gorfman, B. G. Smirnov, G. S. Spirin, and G. N. Shippe, J. Tech. Phys. (U.S.S.R.) **27**, 11 (1957) [Translation: Soviet Phys. (Tech. Phys. **2**, 2471 (1957)].
[11] In. H. Talanin and A. P. Komar, Radiotekhn. i. Elektron. **3**, 1099 (1958); Bull. Acad. Sciences (U.S.S.R.) **22**, 579 (1958).
[12] Yu. V. Zubenkd, A. I. Klimin, and I. L. Sokcl'skaya, Fiz.

Si,[16–20] and Ge.[21–24] Characteristic emission patterns were observed only in some of the more recent investigations (references 11, 17–20, 23, and 24). The results of the current emission measurements were usually given as a plot of the logarithm of the total emitted current versus the reciprocal of the applied voltage since, at least for the case of metals, this yields a straight line. For semiconductors, theory[6] shows that certain deviations from a straight line are possible and qualitative comparisons, between the theoretical predictions and experimental observations, have been made by various authors. (See, in particular, references 13, 16, and 19.) However, since theory relates the emitted current density to the applied field, a detailed knowledge of the emitter tip geometry is required for a quantitative comparison between theory and experiment. Plots of the logarithm of the emitted current density versus the reciprocal of the applied field have been given only in references 14 and 20; most of the other authors quoted assume that the applied field is proportional to the voltage, and the current density to the total current, in their qualitative discussions.

In the present paper the theory presented in I is extended in several ways. The basic equations for the emitted current density are given in Sec. 2 and include a correction which arises if the effective electron mass in the semiconductor differs from the free electron mass. Emission from both the conduction and valence bands are considered. The expression for field emission from the conduction band is simplified in Secs. 3 and 4 following the method of Murphy and Good[25] for metals. The rather complicated conditions given by Murphy and Good, for which these approximate expressions apply, are also presented in a simpler form. Formulas for the emission current, with arbitrary values of the Fermi energy at the surface, are given which reduce to the results for extreme degeneracy or nondegeneracy derived in I.

T-F emission is discussed in Sec. 5. This has previously been considered by Vasil'ev[26] who erroneously compared his result with that for nondegenerate statistics given in I which, however, refers to field emission, i.e., a different range of fields and temperatures. Vasil'ev's result is given in a simpler form for computations; the conditions for *T-F* emission are simplified; and the effective mass correction is derived.

In Sec. 6, a simplified expression for the current density emitted from the valence band is given which will only apply if the hole mass, near the top of the valence band, is considerably less than the free electron mass.

The relation between the Fermi energy at the surface of the semiconductor and the applied field (i.e., field penetration) is discussed in Sec. 7. Detailed results are worked out for simple surface states models and using the surface space charge calculations of Kingston and Neustadter,[27] with their extension to degenerate statistics, for Ge at room temperature, by Seiwatz and Green.[28] These calculations are based on the assumption of a constant Fermi level, i.e., zero current; the conditions under which they may be applied to the present problem, with a non-zero current, are discussed in Appendix III.

Computed field emission curves, taking *n*-type Ge as an example, are discussed in Sec. 8 and compared with experimental data. A treatment for the possible dependence of the field emission current on the hot-electron effect by Elinson[29] is also discussed in Sec. 8.

2. BASIC ELECTRON EMISSION EQUATIONS

Consider an external field F (measured in ev per unit length) applied perpendicular to the surface of a conductor at $x=0$ (cf. Fig. 1). Let ψ be the potential energy required to raise an electron from the bottom of the conduction band, just inside the surface, to a point outside the surface. (The suffix s, which distinguishes energies measured at the surface from those in the interior, will be omitted until Sec. 7). Then, following Nordheim,[30] the probability, that an electron in the conduction band, incident on the surface barrier, emerges from the conductor is given by

$$D(E_x)=\exp\left[-\frac{4}{3}\frac{(2m)^{\frac{1}{2}}}{\hbar}\frac{(\psi-E_x)^{\frac{3}{2}}}{F}v\left(\frac{q\nu F^{\frac{1}{2}}}{\psi-E_x}\right)\right], \quad (1)$$

where $E_x=p_x^2/2m$, $\nu=(\epsilon-1)/(\epsilon+1)^{\frac{1}{2}}$, and electrons in the conduction band are assumed to have the free electron mass. Here, p_x is the x component of the electron momentum $\mathbf{p}$, $-q$ is the charge on the electron, v is a tabulated function[31] involving elliptic integrals which arises from the image force correction, and ϵ is the

Tverd. Tela **1**, 1845 (1959) [translation: Soviet Phys.—Solid State **1**, 1691 (1960)].
[13] G. Busch and T. Fisher, Brown Boveri Review **45**, 532 (1958).
[14] M. I. Elinson and G. F. Vasil'ev, Radiotekhn. i Elektron. **4**, 1718 (1959).
[15] W. Bertoldi and C. Kleint, Ann. Physik **4**, 388 (1959).
[16] Ch. Kleint and R. Fischer, Z. Naturforsch **A14**, 753 (1959).
[17] L. A. D'asaro, J. Appl. Phys. **29**, 33 (1958).
[18] T. Fischer, Helv. Phys. Acta. **33**, 961 (1960).
[19] R. L. Perry, J. Appl. Phys. **32**, 128 (1961).
[20] R. L. Perry (unpublished work).
[21] M. I. Elinson and G. F. Vasil'ev, Radiotekhn. i Elektron. **4**, 728 (1959).
[22] A. I. Klimin, B. N. Sedykh, and I. L. Sokol'skaya, Fiz. Tverd. Tela **2**, 1851 (1960) [translation: Soviet Phys.—Solid State **2**, 1673 (1961).
[23] F. G. Allen, *Proceedings of the International Conference on Semiconductors, Rochester, 1958* [J. Phys. Chem. Solids, **8**, 119 (1959)].
[24] F. G. Allen (unpublished).
[25] E. L. Murphy and R. H. Good, Jr., Phys. Rev. **102**, 1464 (1956).
[26] G. F. Vasil'ev, Radiotekhn. i Elektr. **3**, 962 (1958).
[27] R. H. Kingston and S. F. Neustadter, J. Appl. Phys. **26**, 718 (1955).
[28] R. Seiwatz and M. Green, J. Appl. Phys. **29**, 1034 (1958).
[29] M. I. Elinson, Radiotekhn. i Elektr. **4**, 140 (1959).
[30] L. Nordheim, Proc. Roy. Soc. (London) **A121**, 626 (1928).
[31] R. E. Burgess, H. Kroemer, and J. M. Houston, Phys. Rev. **40**, 515 (1953).

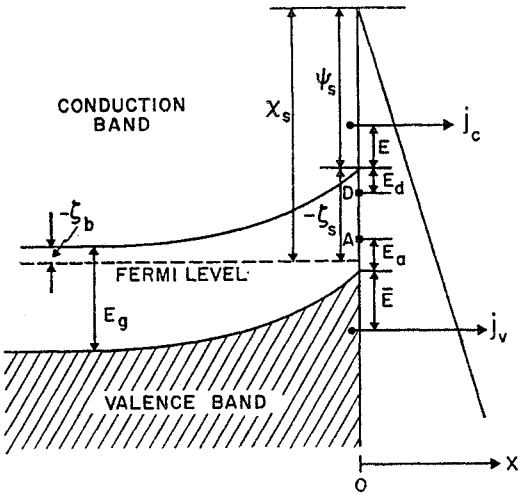

FIG. 1. Electron potential energy diagram of a semiconductor surface showing various energies defined in the text. D and A represent donor and acceptor surface levels. The image force correction is not shown on the figure for the sake of simplicity.

dielectric constant. (The factor ν absent in Nordheim's expression for a metal, gives the image force correction appropriate to a semiconductor.) The expression for $D(E_x)$ is only valid if its magnitude is considerably less than one (I). The condition,

$$D(E_x)<1/e, \tag{2}$$

suggested by Murphy and Good,[25] will be adopted as a suitable criterion.

The restriction to the free electron mass in the conduction band can be removed by replacing E_x with $E(\mathbf{p})-E_\perp$, where

$$E_\perp=(p_y^2+p_z^2)/2m, \tag{3}$$

and $E(\mathbf{p})$ represents the specific dependence of kinetic electron energy on momentum for the conductor. This assumes that the surface potential barrier can be treated as one dimensional and that the tangential component of electron momentum is conserved during the transition, i.e., we merely add the factor $\exp[i(p_y y+p_z z)/\hbar]$ to the wave function in the usual one dimensional calculation involving the W.K.B. approximation.[30] The electron mass occurring in Eqs. (1) [with E_x replaced by $E(\mathbf{p})-E_\perp$] and (3) is that appropriate to free space since the argument of the exponential in Eq. (1) involves an integration over the potential barrier outside the lattice.

The current density emitted from the conduction band is given by

$$j_c=q\frac{2}{h^3}\int\frac{D(E-E_\perp)}{1+\exp[(E-\zeta)/kT]}\frac{\partial E}{\partial p_x}dp_x dp_y dp_z, \tag{4}$$

where ζ is the Fermi energy at the surface, measured from the bottom of the conduction band, and $\partial E/\partial p_x$ is the electron velocity perpendicular to the surface. For spherical energy surfaces (E depends on the magnitude of $\mathbf{p}$ only), the integration over p_y and p_z can be carried out by changing to polar coordinates so that, using Eq. (3),

$$j_c=q\frac{4\pi m}{h^3}\int_0^\infty dE\int_0^{E_m}dE_\perp\frac{D(E-E_\perp)}{1+\exp[(E-\zeta)/kT]}, \tag{5}$$

where $E_m(E)$ is the maximum value of $E_\perp$ for a given value of E. For nonspherical energy surfaces, E_m depends on the polar angle and Eq. (5) would be invalid. The calculation must then proceed from Eq. (4), with the integral evaluated for a definite orientation of the emitting surface.

If the variables of integration E and $E_\perp$ are transformed to E_x and $E_\perp$, where

$$E_x=E-E_\perp, \tag{6}$$

the integration over $E_\perp$ can be performed (cf. Appendix I) and

$$j_c=q(4\pi mkT/h^3)\int_0^\infty dE_x\ln\{1+\exp[(\zeta-E_x)/kT]\}$$
$$\times\{D(E_x)-[1-E_m'(E_x)]D[E_x-E_m(E_x)]\}, \tag{7}$$

where the dash on E_m denotes a derivative. Retaining only the first term $D(E_x)$, inside the second set of curly brackets, leads to the usual expression[25] for the emitted current density (denoted by j_{c0}) based on the free electron mass approximation. The remaining term represents the correction due to an arbitrary dependence of electron energy on scalar momentum. In particular, for a parabolic conduction band with an effective mass m_n, i.e., $E=p^2/2m_n$,

$$E_m(E)=(m_n/m)E, \tag{8}$$

which shows clearly that the correction term vanishes if $m_n=m$. The final integration over E_x will be considered in the next three sections for various ranges of the applied field, temperature, and Fermi energy.

Similarly to Eq. (4), the current density emitted from the valence band is given by

$$j_v=q\frac{2}{h^3}\int\frac{D_v(-\bar{E}+\bar{E}_\perp)}{1+\exp[-(\bar{E}+E_g+\zeta)/kT]}\times\frac{\partial\bar{E}}{\partial\bar{p}_x}d\bar{p}_x d\bar{p}_y d\bar{p}_z, \tag{9}$$

where $\bar{E}$ is the electron energy measured downwards from the top of the valence band (cf. Fig. 1) and $\bar{p}$ is the corresponding momentum, $\bar{E}_\perp$ is defined similarly to $E_\perp$ [cf. Eq. (2)], E_g is the width of the forbidden energy gap and $D_v(E_x)$ is given by the same expression as $D(E_x)$, Eq. (1), except that ψ is replaced by $\psi+E_g$. Again assuming spherical energy surfaces for simplicity

and carrying out the integrations over $\bar{p}_y$ and $\bar{p}_z$ gives

$$j_v=q\frac{4\pi m}{h^3}\int_0^{E_v}d\bar{E}\times\int_0^{\bar{E}_m}d\bar{E}_1\frac{D_v(-\bar{E}+\bar{E}_1)}{1+\exp[-(\bar{E}+E_g+\zeta)/kT]}, \quad (10)$$

where E_v is the valence bandwidth. Making a transformation similar to Eq. (6) and a calculation analogous to that in Appendix I, leads to

$$\begin{aligned}j_v=&q(4\pi mkT/h^3)\\&\times\Big(\int_0^{E_v}d\bar{E}_x\ln\{1+\exp[(\bar{E}_x+E_g+\zeta)/kT]\}\\&\times\{-D_v(-\bar{E}_x)+[1-\bar{E}_m'(\bar{E}_x)]D_v[-\bar{E}_x+\bar{E}_m(\bar{E}_x)]\}\\&+\ln\{1+\exp[(E_v+E_g+\zeta)/kT]\}\\&\times\int_{E_v-\bar{E}_m(E_v)}^{E_v}D_v(-\bar{E}_x)d\bar{E}_x\Big). \quad (11)\end{aligned}$$

The final integration over $\bar{E}_x$ will be considered in Sec. 6.

3. FIELD EMISSION FROM THE CONDUCTION BAND (FREE ELECTRON MASS)

It will now be shown that, for a sufficiently high field F and sufficiently low temperature T, the integral in Eq. (7) can be simplified by expanding the exponent of the exponential factor $D(E_x)$ about either the Fermi level or the bottom of the conduction band. The former is more useful if the Fermi energy is positive, the latter if it is negative. It will however be shown that the approximate expressions are equivalent for small values of the Fermi energy of either sign.

3.1 Positive Fermi Energy

It proves convenient to rewrite the expression for $D(E_x)$ in terms of the constant

$$U=(32/9)(mq^4/\hbar^2)v^4=96.73v^4 \text{ ev}, \quad (12)$$

and the depression of the potential barrier height due to the image force (Schottky effect[32]), i.e.,

$$\psi_i=qvF^{\frac{1}{2}}=3.794\times10^{-4}vF^{\frac{1}{2}} \text{ ev}, \quad (13)$$

where F is in ev cm^{-1}. Thus, from Eq. (1),

$$D(E_x)=\exp\left[-\frac{U^{\frac{1}{2}}(\psi-E_x)^{\frac{3}{2}}}{\psi_i^2}v\left(\frac{\psi_i}{\psi-E_x}\right)\right]\equiv\exp[-B(E_x)]. \quad (14)$$

Expanding the argument, $B(E_x)$, of the exponential about the Fermi level, it can be shown that[25]

$$-B(E_x)=-b_1+c_1(E_x-\zeta)-f_1(E_x-\zeta)^2\cdots, \quad (15)$$

where

$$b_1=B(\zeta)=U^{\frac{1}{2}}\chi^{\frac{3}{2}}v(\psi_i/\chi)/\psi_i^2, \quad (16)$$

$$c_1=\tfrac{3}{2}U^{\frac{1}{2}}\chi^{\frac{1}{2}}t(\psi_i/\chi)/\psi_i^2, \quad (17)$$

$$f_1=\tfrac{3}{8}U^{\frac{1}{2}}v(\psi_i/\chi)[\chi^{\frac{1}{2}}\psi_i^2\{1-(\psi_i/\chi)^2\}]^{-1}, \quad (18)$$

$$t(y)=v(y)-\tfrac{2}{3}ydv(y)/dy, \quad (19)$$

is another tabulated function[5] involving elliptic integrals and χ is the work function ($\chi=\psi-\zeta$, cf. Fig. 1).

Substituting for $D(E_x)$ in Eq. (7), considering only the free electron mass term j_{c0} in the present section, gives

$$j_{c0}=q\frac{4\pi mkT}{h^3}e^{-b_1}\times\int_0^\infty e^{c_1(E_x-\zeta)}\ln\left[1+\exp\left(\frac{\zeta-E_x}{kT}\right)\right]dE_x, \quad (20)$$

provided that the quadratic and higher order terms in the expansion for $B(E_x)$ [Eq. (15)] can be neglected. As a criterion for this, the condition

$$f_1(E_x-\zeta)^2<\tfrac{1}{2}, \quad (21)$$

will be adopted, following Murphy and Good.[25] The limits on F and T, imposed by this condition and inequality (2), will be discussed later. A simple transformation yields

$$j_{c0}=Ae^{-b_1}\int_{e^{-\zeta/kT}}^\infty\nu^{(c_1kT-1)}\ln[1+\nu^{-1}]d\nu, \quad (22)$$

where

$$A=q4\pi m(kT)^2/h^3=120T^2 \text{ amp-cm}^{-2}. \quad (23)$$

Since $\exp(-\zeta/kT)$ is less than one, a more useful form for j_{c0} can be found by using the standard integral[33]

$$p\int_0^\infty\nu^{p-1}\ln[1+\nu^{-1}]d\nu=\pi/\sin p\pi,$$

and integrating by parts, namely,

$$j_{c0}=\frac{Ae^{-b_1}}{(c_1kT)^2}\left[\frac{\pi c_1kT}{\sin(\pi c_1kT)}-e^{-c_1\zeta}(1+c_1\zeta)-G\right], \quad (24)$$

where

$$G=(kTc_1)^2\int_0^{\exp(-\zeta/kT)}\nu^{(c_1kT-1)}\ln(1+\nu)d\nu=(c_1kT)^2e^{-c_1\zeta}\sum_{n=1}^\infty\frac{(-1)^ne^{-n\zeta/kT}}{n(n+c_1kT)}, \quad (25)$$

expanding the integral as a power series in $\exp(-\zeta/kT)$.

[32] W. Schottky, Physik Z. **15**, 872 (1914).

[33] Integrating by parts leads to formula 856.2, H. B. Dwight, *Tables of Integrals*, (The Macmillan Company, New York, 1947), 34th ed.

When T tends to zero, the first term in the square brackets of Eq. (24) tends to one and G tends to zero, yielding our previous result Eq. (I.30) [cf. Eq. (I.24)][6] apart from factors t which we previously replaced by unity. [$t(y)$ increases from one to 1.1107 as y increases from zero to one]. For metals, with a large positive value of the Fermi energy, only the first term in the square brackets of Eq. (24) need be retained in agreement with the result of Murphy and Good. Vasil'ev[26] has derived an expression for j_{c0} which is similar to our Eq. (24) except that G is replaced by two terms involving $\exp[-(c_1\zeta+\zeta/kT)]$ which do not agree with the corresponding term in Eq. (25).

To study the dependence of j_{c0} on the Fermi energy, Eq. (24) will be rewritten as

$$j_{c0}=Ae^{-b_1}H_1(c_1kT,\zeta/kT). \tag{24'}$$

H_1 has been evaluated as a function of c_1kT for various values of ζ/kT, using numerical integrations. The results are shown in Fig. 2 where the numbers on the curves are the values of ζ/kT. The dimensionless quantity c_1kT is essentially inversely proportional to F [cf. Eq. (17)] since $t(y)$ is a slowly varying function of its argument y. Line A in Fig. 2 is drawn parallel to slope of the exponential factor in Eq. (24') for typical values of the parameters, $\chi=4.2$ ev and $\nu=0.94$. [This also neglects the variation of the function $v(y)$.] By comparison with the slopes of the H_1 curves it is evident that the dependence of j_{c0} on F arises mainly from the exponential factor in Eq. (24'). Thus if the work function χ is independent of F, a plot of $\ln j_{c0}$ versus $(1/F)$ will yield an approximately straight line for all positive values of the Fermi energy; any marked deviations from a straight line will only occur if χ changes with F. The numerical analysis has also shown that the asymptotic formula for H_1, obtained by taking only the first term in the series of Eq. (25), is already accurate to about 1%, when ζ/kT equals one.

Murphy and Good have estimated the range of E_z values which give the major contribution to the integral in Eq. (20) and have shown that the two conditions, inequalities (2) and (21), are satisfied if

$$\chi-\psi_i>kT(1-c_1kT)^{-1}+(4\sqrt{2}/3\pi)(\psi_i^{\frac{3}{2}}/U^{\frac{1}{2}}), \tag{26}$$

$$1-c_1kT>kT(2f_1)^{\frac{1}{2}}, \tag{27}$$

respectively [cf. reference 25, Eqs. (57) and (58)]. By a graphical analysis, they further showed that these conditions limit F to a finite range of values provided T is below a certain maximum value. Since the conditions are, however, based on very crude estimates it seems worthwhile to introduce the following further approximations which then yield explicit limits for the allowed range of F values and maximum allowed temperature.

Inequality (26) can be rewritten as

$$\frac{1}{kT}>c_1+\frac{1}{\chi}\left\{1-\frac{\psi_i}{\chi}\left[1+\frac{4\sqrt{2}}{3\pi}\left(\frac{\psi_i}{U}\right)^{\frac{1}{2}}\right]\right\}. \tag{26'}$$

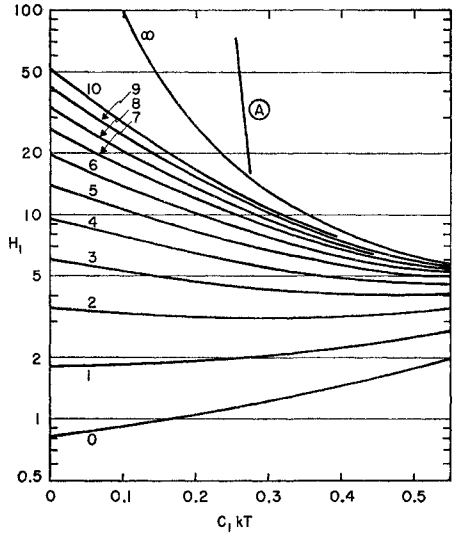

FIG. 2. Dependence of the function $H_1(c_1kT,\zeta/kT)$ on c_1kT for various values of the parameter ζ/kT, marked on the curves. Line A is drawn parallel to the factor $\exp(-b_1)$, in Eq. (24'), for $\chi=4.2$ ev and $\nu=0.94$.

As F increases from zero, c_1 decreases approximately as $(1/F)$ while the second term increases from $(1/\chi)$ and tends to infinity when F satisfies

$$(\psi_i/\chi)[1+(4\sqrt{2}/3\pi)(\psi_i/U)^{\frac{1}{2}}]=1. \tag{28}$$

Thus the right-hand side of inequality (26') has a minimum corresponding to a maximum allowable temperature T_m. For T less than T_m, the inequality will limit F to a finite range of values. If T is well below T_m, the lower limit can be estimated by setting the square bracket equal to one and the upper limit by neglecting c_1. Thus

$$\frac{3U^{\frac{1}{2}}\chi^{\frac{1}{2}}kTt}{2[1-kT/\chi]}<\psi_i^2<\chi^2\left[\frac{1-(kT/\chi)}{1+(4\sqrt{2}/3\pi)(\chi/U)^{\frac{1}{2}}}\right]^2, \tag{29}$$

replacing the small quantity (ψ_i/U) by (χ/U) in the expression for the upper limit. Now each of the factors in the square brackets and the function t are close to unity. Thus, substituting from Eqs. (12), (13), and (17) gives, to a good approximation,

$$2(2m/\hbar^2)^{\frac{1}{2}}\chi^{\frac{1}{2}}kT<F<(\chi/\nu q)^2, \tag{29'}$$

$$2.6\times10^6\chi^{\frac{1}{2}}(T/300)<F<6.95\times10^6(\chi/\nu)^2, \tag{29''}$$

where F is in ev/cm and χ in ev. A more accurate estimate for the limits on F can be obtained by using inequality (29) with the argument of t determined by estimating F from the lower limit of inequality (29').

The lower limit on F, given by inequality (29') is equivalent to our previous estimate derived by a simpler argument [inequality (I.27) with ψ instead of χ for negative Fermi energies, cf. next subsection]. The upper limit is less stringent than our previous estimate [inequality (I.5)] since we took $E_x=0$ in inequality (2)

rather than estimating the largest value of E_x for which it should apply.

The limiting temperature T_m can be derived from inequality (26′) and is approximately given by (assuming $t\approx 1$)

$$\frac{\chi}{kT_m}=\frac{3}{2}\left(\frac{U}{\chi}\right)^{\frac{1}{2}}+2\sqrt{3}\left(\frac{U}{\chi}\right)^{\frac{1}{4}}+\left(\frac{4\sqrt{2}}{\pi}+\frac{3}{2}\right)+O\left[\left(\frac{\chi}{U}\right)^{\frac{1}{4}}\right]. \quad (30)$$

For example, if $\chi=4.5$ ev and $\nu=1$, $T_m\approx 2900°$K. If T is close to T_m, inequality (29) overestimates the allowed range of F values and the original inequality (26) must be used.

Next, the second condition (27), due to Murphy and Good, will be considered, rewritten in the form

$$1/kT>c_1[1+(2f_1)^{\frac{1}{2}}/c_1]. \quad (27')$$

From Eqs. (17) and (18), and using the approximate identity

$$v(y)t^2(y)\approx(1-y^2), \quad (31)$$

given by Murphy and Good[25] [Eq. (65)],

$$(2f_1)^{\frac{1}{2}}/c_1\approx\zeta^{-\frac{1}{2}}t^{-2}(\chi/U)^{\frac{1}{4}}(\psi_i/\chi). \quad (32)$$

Thus substituting from Eq. (17),

$$\psi_i^2>\tfrac{3}{2}U^{\frac{1}{2}}\chi^{\frac{1}{2}}kTt[1+(kT/2\chi)^{\frac{1}{2}}/t], \quad (33)$$

replacing (ψ_i/χ) in the small term inside the square brackets [cf. Eq. (32)] by its lower limit with the square bracket and t replaced by one. Since kT/χ is a small quantity, the lower limit of ψ_i (or F) will be given by inequality (33) rather than inequality (29) although the difference between the two is very small.

The two inequalities (26) and (27) were derived by Murphy and Good for the case of metals, i.e., a large positive Fermi Energy ζ. Actually, it is only required that the integrand of Eq. (20) have its maximum at a value of E_x greater than zero. If the maximum occurs below zero, i.e., outside the range of integration, the important range of E_x above zero can be estimated by requiring that the integrand decreases by about a factor e from its value at $E_x=0$. We then find that the quantity χ in inequality (26) should be replaced by ψ and the factor $(2f_1)^{\frac{1}{2}}$ in inequality (27) should be replaced by $[(1/2f_1)^{\frac{1}{2}}+\zeta]^{-1}$ if ζ is negative. The upper limit on F will become very restrictive when $-\zeta$ approaches $(2f_1)^{-\frac{1}{2}}$. Thus although Eq. (24) for j_{c0} is applicable for small negative values of ζ it is preferable to use another expansion for the integrand in Eq. (7) when ζ is negative.

3.2 Negative Fermi Energy

Expanding $B(E_x)$ [cf. Eq. (14)] about $E_x=0$, rather than $E_x=\zeta$ as in the previous subsection, leads to

$$-B(E_x)=-b_0+c_0E_x-f_0E_x^2\cdots, \quad (34)$$

where b_0, c_0, and f_0 are defined similarly to b_1, c_1, and f_1 [Eqs. (16) and (18)] except that χ is replaced by ψ. Proceeding as in Sec. 3.1 [Eqs. (20) to (25)] we then find

$$j_{c0}=A\exp(-b_0+c_0\zeta)\times\int_0^{\exp(\zeta/kT)}\nu^{-(1+c_0kT)}\ln(1+\nu)d\nu \quad (35)$$

$$=A\exp\left(-b_0+\frac{\zeta}{kT}\right)\times\sum_{n=0}^{\infty}\frac{(-1)^n e^{n\zeta/kT}}{(n+1)(n+1-c_0kT)}, \quad (36)$$

expanding the integral as a power series in $\exp(\zeta/kT)$. Retaining only the first term in the series gives

$$j_{c0}\approx A[\exp(-b_0+\zeta/kT)]/(1-c_0kT)=qn(kT/2\pi m)^{\frac{1}{2}}\exp(-b_0), \quad (36')$$

using the relation between the Fermi energy ζ and electron density n,

$$\exp(\zeta/kT)=n/C_e\equiv\tfrac{1}{2}nh^3/(2\pi mkT)^{\frac{3}{2}}, \quad (37)$$

which applies if $(-\zeta/kT)$ is large compared to one. Apart from the factor $(1-c_0kT)$, which we previously neglected, Eqs. (36′) and (I.29) are equivalent.

The function $H_0(c_0kT,\zeta/kT)$, defined by rewriting Eq. (35) in the form

$$j_{c0}=A\exp(-b_0+\zeta/kT)H_0(c_0kT,\zeta/kT), \quad (36'')$$

has been evaluated as a function of c_0kT for various values of ζ/kT, using numerical integrations. The results are shown in Fig. 3. Comparing with Fig. 2 it will be seen that H_0 varies even less than H_1 as c_0kT (or F) changes so that the dependence of j_{c0} on F will be mainly determined by the exponential factor in Eq. (36″). Similarly to the case of positive Fermi energy energies, any marked deviation from a straight line, on a $\ln j_{c0}$ versus $(1/F)$ plot, will only occur if ζ changes with F. (Note: ψ, being a bulk property, should be independent of F).

A simple extension of the analysis by Murphy and Good shows that the conditions on F are again given by

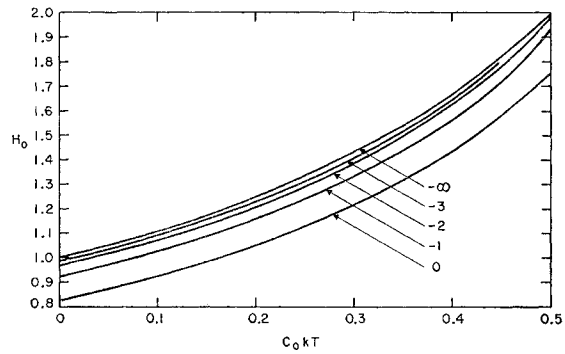

FIG. 3. Dependence of the function $H_0(c_0kT,\zeta/kT)$ on c_0kT for various values of the parameter ζ/kT, marked on the curves.

inequalities (26) and (27) [or their simplified versions (29) and (33)] except that χ must be replaced by ψ wherever it occurs. The two expressions for j_{c0}, derived separately for positive and negative values of ζ, become equivalent for small values of ζ. This can best be seen by comparing Eqs. (22) and (35). The integrals are identically equal and $b_1 \approx b_0 - c_0\zeta$ if $f_0\zeta^2 < \frac{1}{2}$. [Cf. Eq. (15) and inequality (21).]

4. EFFECTIVE MASS CORRECTION

The full expression for the current density j_c emitted from the conduction band [Eq. (7)] will now be considered when the effective mass m_n differs from the free electron mass m [cf. Eq. (8)]. Let

$$\gamma_n = 1 - (m_n/m). \tag{38}$$

Then $D(\gamma_n E_x)$ can be expressed in the form of Eq. (14) for $D(E_x)$ with U, ψ and ψ_i replaced by U', ψ', and ψ_i', respectively, where

$$U' = U/\gamma_n, \quad \psi' = \psi/\gamma_n, \quad \psi_i' = \psi_i/\gamma_n, \quad \text{i.e.,} \quad F' = F/\gamma_n^2. \tag{39}$$

The correction term in Eq. (7) can thus be calculated in the same manner as the leading term j_{c0} in the previous section, by making these replacements, but keeping the Fermi energy ζ and kT unaltered.

Considering the case $\zeta < 0$ first, it can be shown that corresponding to Eq. (39),

$$b_0' = b_0, \quad c_0' = \gamma_n c_0, \quad f_0' = \gamma_n^2 f_0. \tag{40}$$

Thus, using Eq. (36''),

$$j_c = A \exp(-b_0 + \zeta/kT)[H_0(c_0 kT, \zeta/kT) - \gamma_n H_0(\gamma_n c_0 kT, \zeta/kT)]. \tag{41}$$

When $\zeta > 0$, the modified work function,

$$\chi' = \psi' - \zeta = [\chi + (1-\gamma_n)\zeta]/\gamma_n, \tag{42}$$

replaces χ in the correction term. It can further be shown that

$$b_1' = \bar{b}_1, \quad c_1' = \gamma_n \bar{c}_1, \quad f_1' = \gamma_n^2 \bar{f}_1, \tag{43}$$

where the bars on b_1, c_1, and f_1 indicate that χ must be replaced by $[\chi + (1-\gamma_n)\zeta]$ in their definitions [Eqs. (16)–(18)]. Since $(1-\gamma_n)\zeta$ is often considerably less than χ for semiconductors with a partially degenerate surface, the distinction between b_1 and $\bar{b}_1$, etc., can usually be neglected. Using Eq. (24')

$$j_c = A[e^{-b_1} H_1(c_1 kT, \zeta/kT) - \gamma_n \exp(-\bar{b}_1) H_1(\gamma_n \bar{c}_1 kT, \zeta/kT)]. \tag{44}$$

The conditions on F can be deduced by making the necessary substitutions from Eqs. (34), (42), and (43) into conditions (24) and (33).

5. THE INTERMEDIATE RANGE OR $T-F$ EMISSION

It will now be assumed that most of the emitted electrons come from energy levels well above the Fermi level but still below the top of the barrier so that they must tunnel through the barrier, rather than going over it as in thermionic emission. It will shortly be shown that this occurs for fields which are below the lower limit for field emission, discussed in Sec. 3.

Vasil'ev[26] has already derived the expression for the emitted current density j_{c0} (assuming the free electron mass) for this intermediate range. The calculation will be briefly repeated for three reasons. First, the final expression for j_{c0} will be given in a form more amenable to numerical evaluation than Vasil'ev's expression. Then the very complicated conditions for the intermediate range given by Vasil'ev, following Murphy and Good,[25] will be simplified, leading to explicit expressions for the upper and lower limit on the field. This shows clearly that Vasil'ev's comparison of his result with the present author's earlier field emission calculation is irrelevant since the two results apply in different field ranges. Finally the effective mass correction for the emitted current density will be derived.

The emitted current density from the conduction band, assuming a free electron mass for the present is given by [cf. Eqs. (7) and (14)]

$$j_{c0} = q\frac{4\pi mkT}{h^3} e^{\zeta/kT} \int_0^\infty \exp\left[-\frac{E_x}{kT} - B(E_x)\right] dE_x, \tag{45}$$

if

$$\exp[(E_x - \zeta)/kT] \gg 1. \tag{46}$$

The integrand will have a maximum at a value E_m of E_x which satisfies the equation [cf. Eq. (15)]

$$c_m kT = 1, \tag{47}$$

where c_m is given by Eq. (17), for c_1, with χ replaced by $(\psi - E_m)$. From inequality (46) it follows that c_m must be less than c_1. Thus Eq. (47) will only be satisfied if $c_1 kT$ is greater than one. This is essentially the converse of the previous condition which gave the lower limit on F [cf. inequality (27')] for field emission.

Expanding about $E_x = E_m$ gives

$$B(E_x) + E_x/kT = b_m + c_m E_m + f_m(E_x - E_m)^2 \cdots, \tag{48}$$

where b_m and f_m are given by Eqs. (16) and (17) with χ replaced by $\psi - E_m$. Substituting into Eq. (45) then leads to

$$j_{c0} = \frac{A}{2kT} \exp\left(\frac{\zeta}{kT} - b_m - \frac{E_m}{kT}\right) \times \left(\frac{\pi}{f_m}\right)^{\frac{1}{2}} \{1 + \operatorname{erf}(E_m f_m^{\frac{1}{2}})\}. \tag{49}$$

This is equivalent to Vasil'ev's[26] Eq. (15) as may be

verified by substituting for f_m from Eq. (18) [using Eq. (31)], $\exp\zeta/kT$ from Eq. (37), U from Eq. (12), ψ from Eq. (13), and A from Eq. (23). {Vasil'ev's statement that if $E_m=0$, Eq. (49) reduces to our earlier result (1.29) [cf. Eq. (36')] is incorrect due to the additional factor $[(\pi/f_0)^{\frac{1}{2}}/2kT]$ which then occurs in Eq. (49).}

Explicit values of j_{c0} for a given value of F and T can be derived by solving Eq. (47) for E_m and substituting into Eq. (49) or Vasil'ev's result. A more useful form of Eq. (50) can be derived by introducing the dimensionless quantity

$$P^2=(4/27)\psi_i^4[U(kT)^3]^{-1}\propto F^2/T^3. \tag{50}$$

Then

$$f_m^{\frac{1}{2}}=[2(3t_m)^{\frac{1}{2}}kTP]^{-1}, \tag{51}$$

$$E_m=\psi-3kTP^2/t_m^2, \tag{52}$$

$$b_m=2(v_m/t_m^3)P^2, \tag{53}$$

using Eqs. (16)–(18), (31), and (47). Substituting into Eq. (49) then gives

$$j_{c0}=A(3\pi t_m)^{\frac{1}{2}}P\exp\{-(\chi/kT)+P^2\theta_m\}\times[1+\mathrm{erf}\{[(\psi/kT)-(3P^2/t_m^2)]/2P(3t_m)^{\frac{1}{2}}\}], \tag{54}$$

where the function

$$\theta(y)=3t^{-2}(y)-2v(y)t^{-3}(y), \tag{55}$$

has been tabulated by Murphy and Good.[25] The suffix m on t and θ denotes that these quantities have the argument

$$y_m=\psi_i/(\psi-E_m). \tag{56}$$

For a given value of P, y_m can be determined by combining Eqs. (50) and (52) in the form

$$t_m^2/y_m=P^{\frac{2}{3}}(12kT/U)^{\frac{1}{3}}. \tag{57}$$

The advantage of Eq. (54) over Eq. (49) is that, since θ_m and t_m are slowly varying functions of y_m, the solution of the subsidiary Eq. (57) need not be known with great accuracy. Use of Eq. (49) however requires an accurate solution for E_m from the subsidiary Eq. (47).

It will shortly be shown that the argument of the error function in Eq. (54) is large if the Fermi energy is large. The error function can then be replaced by one and Eq. (53) reduces to the result for metals given by Murphy and Good.[25] [Their Eq. (75).] Since the error function lies between zero and one for any value of the Fermi energy, j_{c0} is approximately proportional to the exponential factor. Thus, if χ is independent of F, a plot of $\ln j_{c0}$ versus F^2 will give an approximately straight line since θ_m is a slowly varying function. Alternatively, a plot of $\ln j_{c0}$ versus $(1/F)$ will give a curve which is convex towards the origin.

Murphy and Good[25] have shown that the conditions for which inequalities (2) and (46) will be satisfied are approximately

$$\psi-E_m>\psi_i+kTd^2(d-1)^{-1}, \tag{58}$$

where

$$d=\frac{4\sqrt{2}}{3\pi}\frac{\psi_i^{\frac{3}{2}}}{U^{\frac{1}{2}}kT}=\frac{2\sqrt{2}}{\pi}\frac{t_m(\psi-E_m)^{\frac{1}{2}}}{\psi_i^{\frac{1}{2}}}, \tag{59}$$

and

$$\chi>\chi g^2/t_m^3+kT(1-g/t_1)^{-1}, \tag{60}$$

where

$$g=\tfrac{2}{3}\psi_i^2/U^{\frac{1}{2}}kT, \tag{61}$$

respectively [cf. reference 26, inequalities (62) and (69); t_1 is the value of $t(y)$ when $y=\psi_i/\chi$]. These will now be further simplified by making additional approximations.

Eliminating $(\psi-E_m)$ between inequality (58) and Eq. (59) leads to

$$[(\pi^2/8t_m^2)d^2-1](d-1)d^{-\frac{1}{2}}>l, \tag{62}$$

where

$$l=(4\sqrt{2}/3\pi)^{\frac{1}{2}}(kT/U)^{\frac{1}{4}}, \tag{63}$$

is a small dimensionless quantity equal to about 0.05 at room temperature. The left-hand side of inequality (62) is positive if d is less than $2\sqrt{2}t_m/\pi$ or greater than one and negative if d is between these roots. Now t_m is itself a function of d; its argument is $8t_m^2/\pi^2d^2$ [cf. Eq. (54)]. Thus when d equals $2\sqrt{2}t_m/\pi$, the argument of t_m is one, so that $t_m=1.1107$ and the corresponding value of d is 1.0001. Hence the two roots actually coalesce at $d=1$ and inequality (62) will be satisfied if

$$d>1+(\tfrac{1}{2}l)^{\frac{1}{2}}+O(l). \tag{64}$$

[The other possibility, $d<1-(\frac{1}{2}l)^{\frac{1}{2}}$, can be rejected since it implies $\psi_i>\psi-E_m$ which is impossible.] Substituting from Eqs. (12), (13), (59), and (63) gives

$$F>\left(\frac{\pi^2mqk^2\nu}{\hbar^2}\right)^{2/3}T^{4/3}\left[1+\frac{4}{3\sqrt{2}}\frac{\hbar^{1/3}k^{1/6}T^{1/6}}{\pi^{1/3}m^{1/6}q^{2/3}\nu^{2/3}}\right], \tag{65}$$

or

$$F>2.2\times10^6\nu^{2/3}(T/300)^{4/3}[1+0.21(T/300)^{1/6}/\nu^{2/3}],$$

where F is in ev/cm:

The second condition given by Murphy and Good [inequality (59)] can be rewritten as

$$(g+t_m)(g-t_m)(g-t_1)/t_m^2t_1>kT/\chi. \tag{66}$$

Let $t_m+\delta$ be the value of g for which the two sides of this inequality are equal. Then

$$(kT/\chi)=2\delta(t_m-t_1)/t_mt_1+\delta^2(3t_m-t_1)/t_m^2t_1+O(\delta^3), \tag{67}$$

(Note: kT/χ is always small). In Appendix II it is shown that (t_m-t_1) is considerably less than δ and that δ is negative. Hence inequality (60) will be satisfied if

$$g<t_m-t_m(kT/2\chi)^{\frac{1}{2}}+O(kT/\chi). \tag{68}$$

{The other possibility, $g>t_m+t_m(kT/2\chi)^{\frac{1}{2}}$, can be rejected since g is approximately equal to $(1/c_1kT)$ [cf. Eq. (17)] which must be less than one as pointed out in connection with Eq. (47).} Substituting from Eq. (61) gives

$$\psi_i^2<\tfrac{3}{2}U^{\frac{1}{2}}\chi^{\frac{1}{2}}kTt_m[1-(kT/2\chi)^{\frac{1}{2}}], \tag{69}$$

i.e., essentially the inverse of the condition [inequality (33)] which gives the lower limit on F for the field emission range [cf. Eq. (29′) for the explicit condition on the field].

The quantity P [Eq. (50)] is equal to $(\chi/3kT)^{\frac{1}{2}}g$ [cf. Eq. (61)]. Since g is approximately less than one, the argument of the error function in Eq. (54) will be greater than about $\frac{1}{2}\zeta(\chi kT)^{-\frac{1}{2}}$. For metals this quantity is sufficiently large to make the error function equal one as was implicitly assumed by Murphy and Good.

The two basic inequalities (58) and (60), quoted from reference 26, were derived for metals. Inequality (58) [or its simplified version (65)] actually holds for all values of the Fermi energy. For a sufficiently large negative value of the Fermi energy, inequality (46), will be satisfied for all values of the field. The upper limit on F will then be given by the condition that E_m must be greater than zero. From Eq. (52) [using Eq. (50)] it can be seen that this merely requires that χ be replaced by ψ in inequality (69), the term in square brackets being omitted.

The complete expression for the emitted current density j, including the effective mass correction, can be derived by replacing the parameters in Eq. (54) according to the prescription in Sec. 4 [Eqs. (34) and (42)]. In particular

$$P'=P/\gamma_n^{\frac{1}{2}}, \tag{70}$$

and if Eq. (54) is rewritten as

$$j_{c0}=AH_2[\chi/kT,\psi/kT,P], \tag{71}$$

then

$$j=A\{H_2[\chi/kT,\psi/kT,P] -\gamma_n H_2[\{\chi+(\gamma_n-1)\zeta\}/\gamma_n kT,\psi/\gamma_n kT,P/\gamma_n^{\frac{3}{2}}]\}. \tag{72}$$

6. FIELD EMISSION FROM THE VALENCE BAND

It will first of all be assumed that the hole Fermi level at the surface is several kT above the top of the valence band, i.e., $(E_g+\zeta)/kT$ is considerably greater than one and the hole distribution is non-degenerate. If further $\bar{E}_m(\bar{E}_x)$ is sufficiently small compared to $\bar{E}_x$, then the first integral in Eq. (11) is over a region near the top of the valence band, and the upper limit E_v may be taken as infinity, since $D_v(-\bar{E}_x)$ decreases very rapidly as $\bar{E}_x$ increases from zero. Similarly, the second integral, which is over a region near the bottom of the valence band, may be neglected. We thus assume that

$$\bar{E}_m(\bar{E}_x)=(m_p/m)\bar{E}_x, \quad m_p/m<1, \tag{73}$$

where m_p is the effective hole mass near the top of the valence band, the only region from which electron emission is important. Expanding about $\bar{E}_x=0$,

$$D_v(-\bar{E}_x)=\exp(-b_v-c_v\bar{E}_x-f_v\bar{E}_x^2\cdots), \tag{74}$$

where b_v, c_v, and f_v are given by Eqs. (16), (17), and (18) for b_1, c_1, and f_1, with χ replaced by $\psi+E_g$. Substituting into Eq. (11), taking $\gamma_p=1-m_p/m$, gives

$$j_v=Ae^{-b_v}\int_0^\infty d\bar{E}_x(\bar{E}_x+E_g+\zeta)/(kT)^2 \times[-\exp(-c_v\bar{E}_x)+\gamma_p\exp(-\gamma_p c_v\bar{E}_x)], \tag{75}$$

provided that

$$f_v\bar{E}_x^2<\tfrac{1}{2}. \tag{76}$$

Thus, evaluating the integral

$$j_v=Ae^{-b_v}(c_vkT)^{-2}(\gamma_p^{-1}-1). \tag{77}$$

Since A is proportional to T^2, j_v is independent of temperature as would be expected.

The main contribution to the integral in Eq. (75) comes from values of $\bar{E}_x$ in the range 0 to $(1/\gamma_p c_v)$. Thus inequality (76) will be satisfied if

$$(2f_v)^{\frac{1}{2}}<c_v\gamma_p, \tag{78}$$

or, substituting from Eqs. (12), (13), (17), (18), and (31), if

$$F<4(2m/\hbar^2)^{\frac{1}{2}}t_v^4\gamma_p^2(\psi+E_g)^{\frac{1}{2}} \tag{78′}$$

$$<2.0\times10^8t_v^4\gamma_p^2(\psi+E_g)^{\frac{1}{2}}, \tag{78″}$$

where F is in ev/cm and $\psi+E_g$ in ev.

If (m_p/m) is not less than one, contributions from lower lying portions of the valence band cannot be neglected. The calculation for j_v then requires a detailed knowledge of the relation between electron energy and momentum over an appreciable portion of the valence band.

The calculation has only been carried out for a completely filled valence band since only the rather unlikely occurrence of a strongly degenerate p-type surface would lead to a result substantially different from Eq. (77). It would however be an easy matter to extend the calculation, for an arbitrary Fermi energy, along similar lines to Sec. 3. In particular, for a degenerate p-type surface, the predominant exponential factor in Eq. (77) would have b_v replaced by b_1 [cf. Eq. (16)].

It seems reasonable to suppose that emission from the valence band will predominate over that from the conduction band if the Fermi energy is large and negative (few electrons in the conduction band) and vice versa if the Fermi energy is large and positive. It is however not possible to give a simple criterion for the Fermi energy at which the two emissions will be comparable due to the complicated dependence of the two emission currents on various parameters.

An approximate derivation by Morgulis (cf. reference 6) gave j_v proportional to $\exp(-b_v^1)$, where b_v^1 differs from b_v [cf. Eq. (77)] by having $\psi+E_g+\frac{1}{2}\alpha E_v$ instead of $\psi+E_g$ in the defining Eq. (16). (The coefficient of proportionality was not evaluated.) The parameter α was taken as approximately one.

7. SURFACE SPACE-CHARGE REGION

In the previous sections, the emitted current density was derived in terms of the Fermi energy and work function at the surface of the semiconductor. The relation between these parameters (written with a suffix s in future) and the bulk parameters of the semiconductor will now be considered. Let F_s be the internal field at the surface, taken as positive if it acts in the opposite direction to F. Then

$$F+\epsilon F_s=-4\pi q\sigma_s, \tag{79}$$

where σ_s is the surface charge density arising from surface states. It is also useful to introduce the following special values of F, F_s, and σ_s, namely,

$$\epsilon F_{s0}=-4\pi q\sigma_{s0}, \tag{79a}$$

and

$$F_1=-4\pi q\sigma_1, \tag{79b}$$

the latter giving the flat band condition.

The expressions for the emitted current density from the conduction band involve the Fermi energy ζ_s, at the surface as a parameter. If F_s and σ_s are known as functions of ζ_s, then ζ_s can be calculated from Eq. (79), for a given value of F. The dependence of F_s and σ_s on ζ_s will be derived on the assumption that the Fermi level, for both electrons and holes, does not change appreciably in the space charge region and also defines the occupancy of the surface states. This assumption is discussed in Appendix III where it is shown that it should apply for semiconductors whose bulk electron density is sufficiently high and in the absence of field emission from the surface states. (It is intended to investigate other cases, where the assumption does not apply, in future work.)

With the assumption of a constant Fermi level it is possible to derive the relation between F_s and ζ_s by solving Poisson's equation in the space-charge region. In Paper I we considered an n-type semiconductor and neglected the contribution to the space charge from holes. This is reasonable for a material with a large energy gap such as SiC [$E_g=2.9$ ev(α) or 2.2 ev(β)], which was chosen as an example for the computations. Detailed results were only worked out for the extreme cases corresponding to $|\zeta_s-\zeta_b|/kT$ very much greater than one. (ζ_b is the value of the Fermi energy in the bulk material.) In the present paper we consider the calculation for arbitrary values of ζ_s and also include the space charge contribution due to holes which is important for materials with narrower energy gaps such as Si and Ge. Following Kingston and Neustadter,[27] the relation between F_s and ζ_s can be written in the form

$$F_s=(kT/L_D)F_{KN}(u_b,u_s), \tag{80}$$

where

$$u_b=(\zeta_b-\zeta_i)/kT,\quad u_s=(\zeta_s-\zeta_i)/kT,\quad L_D=(\epsilon kT/8\pi q^2 n_i), \tag{81}$$

is the Debye length, n_i is the electron density, ζ_i the Fermi energy of the intrinsic semiconductor, and $F_{KN}(u_b,u_s)$ has been computed for various values of the arguments. (See reference 34 for an extension of Kingston and Neustadter's computed results to higher values of u_b and u_s.) Equation (80) only applies if the free carrier distributions are nondegenerate and if the impurities are fully ionized. This requires that $-\zeta_s$, $E_g+\zeta_s$ and the separation between each impurity level and the Fermi level, are all greater than about $3kT$. Seiwatz and Green[28] have extended the calculations by removing these restrictions. It is then not possible to derive F_s from a universal function as in Eq. (80); the energy gap, impurity levels, density of states masses and the temperature must be specified. As an example, Seiwatz and Green[28] considered n-type Ge at 300°K [donor activation energy 0.1 ev, $E_g=0.65$ ev, $(m_n/m)^{\frac{3}{2}}=0.412$, $(m_p/m)^{\frac{3}{2}}=0.216$] and calculated F_{KN}, as defined by Eq. (80), for this specific case. It turns out that the value of F_{KN} is approximately independent of u_b if $0\leq u_b\leq 6$ and $|u_s|>12$. The computed field emission curves, presented in the next section, are based on the particular parameters assumed by Seiwatz and Green[28] so that the results of their calculation may be used.

For extreme degeneracy, i.e., when ζ_s/kT is very much greater than one, the simple relation, previously derived in I.

$$\zeta_s=\lambda(\epsilon F_s)^{4/5},$$
$$\lambda=\frac{1}{8}\left(\frac{15}{2\epsilon}\right)^{2/5}\frac{h^{6/5}}{m_n^{3/5}q^{4/5}}=\frac{(m/m_n)^{3/5}}{\epsilon^{2/5}}4.708\times10^{-7}\ \text{ev}^{1/5}\ \text{cm}^{4/5}, \tag{82}$$

may be used.[35] The values of ζ/kT for which this equation is reasonably accurate can be estimated by comparing with the exact result given by Seiwatz and Green.[28] For a given value of F_s, ζ_s, deduced from Eq. (82), will be too large, by less than 6%, if ζ_s/kT is greater than about 3 (Note: $\zeta_i/kT=-12.9$). However, for a given value of ζ_s, F_s deduced from Eq. (82) will be too small, by about 40% if ζ_s/kT is about 3. For a better than 6% accuracy in this case, ζ_s/kT must be greater than about 9.

The surface charge density is given by

$$\sigma_s=q[(N_d-n_d)-(N_a-p_a)], \tag{83}$$

where N_d is the density of donor type surface states, occupied by n_d electrons and N_a is the density of acceptive type surface states, occupied by p_a holes. In general, the right-hand side of Eq. (83) will be summed

[34] C. E. Young, J. Appl. Phys. 32, 324 (1961).

[35] The value of λ given by Eq. (I.25) or contains arithmetical errors. Also the first factor 2 in Eq. (I.18) should be deleted and the following numerical factors should be replaced: 16 by 8 in Eqs. (I.25) and (I.26), 0.78 by 0.55 in Eq. (I.26) and 1.2×10^6 by 8.6×10^5 in Eq. (I.26a).

TABLE I. Parameters selected for the calculated dependence of the Fermi energy at the surface on the applied field (see Figs. 4 and 5).

F_1 (10^7 ev/cm)	$(\zeta_{s0}-\zeta_b)/kT$	F_{s0} (10^5 ev/cm)	N_a (10^{13} cm^{-3})	E_a/kT	ψ_s/kT
1	−12	1.65	0.55	9.4	165
3	−7	1.81	1.83	16.0	170
3	−12	0.26	1.67	10.6	165
3	−18	1.65	1.67	2.6	159
5	−12	1.65	2.66	11.1	
3.95	−18.8	2.4	···	···	158

or integrated over a discrete or continuous distribution of surface levels, respectively. The quantities n_d and p_a are given by

$$n_d/N_d=[1+\exp\{-(\zeta_s+E_d)/kT\}]^{-1}, \quad (84)$$

$$p_a/N_a=[1+\exp\{(\zeta_s+E_g-E_a)/kT\}]^{-1}, \quad (85)$$

where E_d is the donor and E_a the acceptor surface state activation energy (cf. Fig. 1). (These are effective activation energies which include a term kT ln$g$, where g is a measure of the state degeneracy. For a doubly degenerate center, g equals 0.5.)

The surface states model considered in I consisted of a single donor and a single acceptor level with $(E_g+\zeta_s-E_a)/kT$ always greater than one so that p_a was zero. In the present paper two alternative distributions of surface levels are considered which may apply for a clean Ge surface.[36–38]

First only a single acceptor surface level will be assumed. Then from Eqs. (79), (83), and (85)

$$\sigma_s=-qN_a[1+\exp\{(E_a-E_g-\zeta_s)/kT\}]^{-1}, \quad (86)$$

$$\frac{F+\epsilon F_s}{F_{s0}}=\frac{\sigma_s}{\sigma_{s0}}=\frac{1+\exp\{(E_a-E_g-\zeta_{s0})/kT\}}{1+\exp\{(E_a-E_g-\zeta_s)/kT\}},$$

$$\frac{F_1}{\epsilon F_{s0}}=\frac{\sigma_{s1}}{\sigma_{s0}}=\frac{1+\exp\{(E_a-E_g-\zeta_{s0})/kT\}}{1+\exp\{(E_a-E_g-\zeta_b)/kT\}}, \quad (87)$$

where ζ_{s0} is the value of ζ_s when $F=0$. As a specific example, n-type Ge, at room temperature, will be considered with u_b equal to 6, or $\zeta_b/kT=-6.9$, i.e., a bulk electron density of about 10^{16} cm^{-3}. If ζ_{s0} and F_1 are also specified, ζ_s can be evaluated as a function of F from Eqs. (80) (using references 27 and 28) and Eq. (87). The three values of F_1 selected (cf. Table I) are such that the electron distribution at the surface is either nondegenerate ($F_1=5\times10^7$ ev/cm), degenerate ($F_1=1\times10^7$ ev/cm) or changes from nondegenerate to degenerate ($F_1=3.10^7$ ev/cm) as F increases from 2 to 4×10^7 ev/cm, the range for which field emission currents will

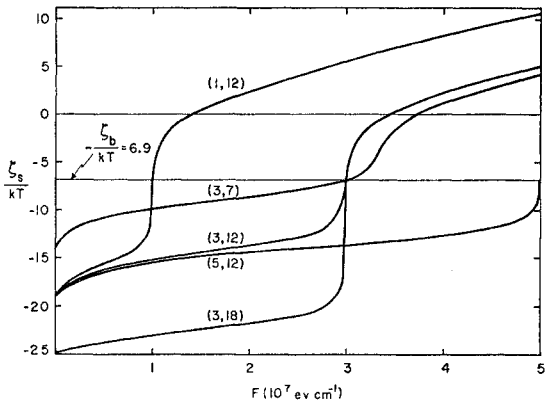

FIG. 4. Dependence of the reduced Fermi energy at the surface (ζ_s/kT) on the applied field F for a single surface acceptor level. The numbers, in parenthesis, on the curves refer to the value of F_1 and $(\zeta_{s0}-\zeta_b)/kT$ respectively, for the five cases listed in Table I. Calculation for n-type germanium at room temperature.

be calculated. The calculated dependence of ζ_s/kT on F, for each of the five cases listed in Table I, is shown in Fig. 4. The effect of different initial barrier heights is illustrated by the three values of $(\zeta_{s0}-\zeta_b)/kT$ chosen in association with $F_1=3\times10^7$ ev/cm. (The curves for the two higher barriers coincide for fields greater than that for the flat band conditions). The rapid variation of ζ_s, when F is near F_1 becomes more pronounced as the initial barrier height is increased. The two cases corresponding to $F_1=1\times10^7$ ev/cm and $F_1=5\times10^7$ ev/cm have been worked out for only one initial barrier height each; the shape of the curves for other barrier heights will be similar to those for $F_1=3\times10^7$ ev/cm except for the different values of F for which the flat band condition occurs.

As is to be expected, the first point of inflexion, as F increases from zero, on each of the curves, occurs for a value of ζ_s close to E_g-E_a, i.e., when the Fermi level coincides with the surface state level.

The derived quantities F_{s0} [from Eq. (80)], E_a/kT [from Eq. (87a) using $E_g/kT=25.2$], and N_a [from Eqs. (79a) and (86)] are also listed in Table I. (The column ψ_s/kT will be discussed in the next section.) The flat band condition will only occur in the selected field emission range if N_a is about 2×10^{13} cm^{-2}. (This conclusion is not confined to n-type Ge.) If N_a is greater than about 2×10^{13} cm^{-2}, any initial internal surface barrier is sustained, although somewhat lowered, in the field emission range. If N_a is less than about 1×10^{-13} cm^{-2}, field penetration will lead to a degenerate accumulation region at the surface, the value of ζ_s, being only slightly dependent on the value of N_a.

Next, a continuous distribution, or band of acceptor surface levels will be considered. Then

$$\sigma_s=-q\int_{E_{a1}}^{E_{a2}}[1+\exp\{(E_a+E_g-\zeta)/kT\}]^{-1}\times\mathfrak{N}(E_a)dE_a, \quad (88)$$

[36] W. Portnoy and P. Handler, University of Illinois, Electrical Engineering Research Laboratory, Technical Report No. 2, 1959 (unpublished).
[37] P. Handler and W. Portnoy, Phys. Rev. **116**, 516 (1959).
[38] P. Handler, J. Phys. Chem. Solids **14**, 1 (1960).

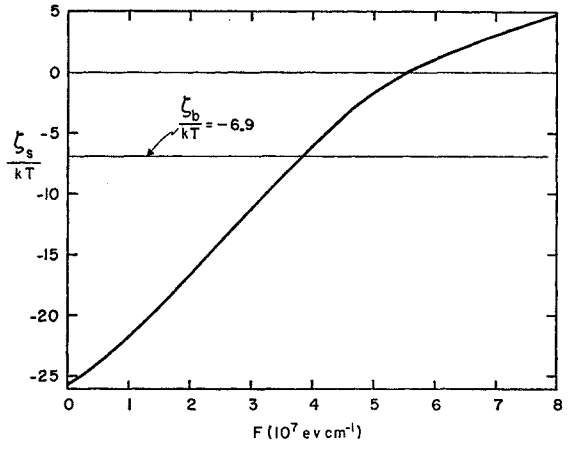

FIG. 5. Dependence of the reduced Fermi energy at the surface (ζ_s/kT) on the applied field F for the surface states model proposed by Handler,[38] for n-type germanium at room temperature.

where $\mathfrak{N}(E_a)$ is the density of states per unit energy and the band edges are at E_{a1} and E_{a2}. Such a model has been suggested for Ge,[38] with $\mathfrak{N}(E_a)$ assumed to be constant and equal to about 4×10^{13} cm^{-2} ev^{-1} and $(-E_{a1}+E_g+\zeta_{s0})/kT$ approximately equal to 2. Thus, taking the upper limit as infinity,

$$\sigma_s=-q\mathfrak{N}kT\ln[1+\exp(\zeta_s+E_g-E_{a1})/kT]. \quad (89)$$

Proceeding as for the previous case of a single level leads to the derived parameters in the last line of Table I and the dependence of ζ_s on F, shown in Fig. 5. Since the flat band condition occurs near the upper limit of the previously selected field emission range, the calculation has been extended to higher values of F. By comparing Figs. 5 and 6 it can be seen that the continuous distribution of surface states leads to a far more gradual variation of ζ_s as F passes through the flat band condition.

8. RESULTS AND DISCUSSIONS

The field emission current j_c from the conduction band, for a given value of the applied field F, was derived in Secs. 3 and 4 in terms of a field-dependent surface Fermi energy (ζ_s) or work function (χ_s). Thus, with the results of the last section, j_c can be evaluated as a function of F. Besides the parameters required for the surface space charge calculation, (bulk Fermi energy, impurity level, energy gap, density of states masses, dielectric constant, and temperature), the conduction band edge potential ψ_s (cf. Fig. 1) and a suitable effective electron mass, for the tunneling probability, must be specified.

Figures 6 and 7 show computed conduction band field emission curves based on the particular example of n-type Ge considered by Seiwatz and Green[28] in their surface space-charge calculation. The effective mass which enters into the tunneling probability, calculated for spherical energy surfaces in Sec. 2, has been assumed equal to the inertial mass[39] of the ellipsoidal, conduction band, energy surfaces[40] of Ge, i.e. $m_n/m=0.12$. Various experimental determinations of the work function, (χ_{s0}) for a Ge surface, produced either by cleaving in a high vacuum,[41] or by argon ion bombardment,[42] or by evaporation of a film onto a metallic substitute,[43] all gave values close to 4.75 ev. No appreciable variation in χ_{s0} was observed for a wide range of doping levels and temperatures.[44] This indicates that a sufficiently large density of surface states was primarily responsible for the magnitude of χ_{s0}. Since χ_{s0} equals $\psi_s-\zeta_{s0}$, the value of ψ_s was taken as $(4.75+\zeta_{s0})$ ev, for each of the examples listed in Table I.

Field emission curves for the case of a single, acceptor surface level are shown in Fig. 6. Curve (18,3), which shows a rapid increase in j_c as F increases though the value of F_1 (flat band condition), is similar to our previously calculated (cf. I) field emission curve. The rapid increase in j_c, for F near F_1, is progressively reduced in curves (12,3) and (7,3) as the initial barrier height is lowered. This reflects the similar behavior of the Fermi energy at the surface (cf. Fig. 4). Curves (12,1) and (12,5) are essentially straight lines since neither χ_s nor ζ_s, respectively, are rapidly changing functions of F. [The fact that curve (12,1) is actually a straight line, to the accuracy of the figure, is accidental and depends on the particular set of parameters assumed.] The shape of the five curves beyond the range of fields considered in

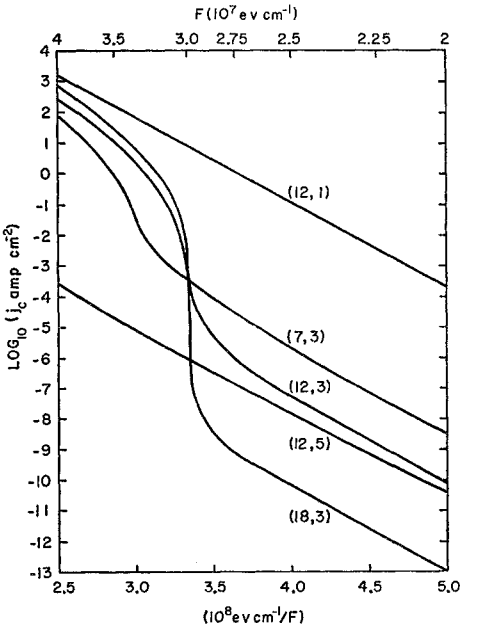

FIG. 6. Conduction band field emission curves [$\log j_c$ versus $(1/F)$] for a single surface acceptor energy level. The numbers, in parenthesis, on the curves refer to the value of F_1 and $(\zeta_{s0}-\zeta_b)/kT$ respectively, for the five cases listed in Table I calculation for n-type germanium at room temperature.

[39] C. Herring, Bell System Tech. J. 34, 237 (1957).
[40] F. Herman, Proc. Inst. Radio Engrs. 43, 1703 (1957).
[41] D. Haneman, J. Phys. Chem. Solids 11, 205 (1959).
[42] J. A. Dillon, Jr., and H. E. Farnsworth, J. Appl. Phys. 28, 174 (1957).
[43] L. Apker, E. Taft, and J. Dickey, Phys. Rev. 74, 1462 (1948).
[44] F. G. Allen, Ph.D. thesis, Howard University, 1955 or Cruft Laboratory Technical Report No. 237, (unpublished).

Fig. 6, is obvious. Curve (12,1) decreases sharply for smaller F, near $F=1\times10^7$ ev/cm and curve (12,5) increases sharply for larger F, near $F=5\times10^7$ ev/cm. In the opposite direction both curves, and all the other curves, continue as approximately straight lines.

The field emission curve for the case of a linear distribution of surface states is shown in Fig. 7. Just as for the case of a single surface level, there is a point of inflexion for F near F_1. However, the variation of the slope is far more gradual than for the curves, with $F_1=3\times10^7$ ev/cm, in Fig. 6. More complicated distributions of surface states, than either of the simple cases treated in this paper, will lead to correspondingly more complicated field emission curves which may show more than one point of inflexion.

The field emission current from the valence band in Ge has been calculated from Eq. (77) and is also plotted in Fig. 7. Contributions from light-hole mass ($m_p/m=0.043$) and heavy-hole mass ($m_p/m=0.35$) states have been added together, the former being predominant.

By comparing Figs. 6 and 7, it will be seen that, for our model of Ge, field emission from the valence band predominates over field emission from the conduction band except when F_1 (or the surface states density N_a) is sufficiently low to permit strong field penetration, as exemplified by curve (12,1) in Fig. 6. The calculated conduction band field emission curves, for the other cases, have nevertheless been presented in detail since they are of interest for other semiconductors, with a wider energy gap than Ge.

The most reliable experimental determination of field emission from a clean Ge surface is that due to Allen[24] who observed the characteristic symmetrical pattern. He was, however, unable to determine the geometry of the Ge emitter tip so that his experimental results are given as the dependence of the total emitted J on the applied voltage V. Allen finds that[24]

$$I=C\exp(-W/V), \tag{90}$$

where $C=32$ amp and $W=9.4\times10^4$ v. We now make a crude estimate to see whether Allen's data are consistent with field emission from the valence band. For the latter one can write

$$j_v=c\exp(-w/F), \tag{91}$$

where $c=5.8\times10^{10}$ amp-cm^{-2}, and $w=7.3\times10^8$ ev-cm^{-1}, can be determined from Fig. 7. In the absence of any information about the emitter geometry, it will be assumed that

$$V/F=W/w=r/\beta, \quad I/j=r^2\Omega=C/c, \tag{92}$$

where r is the (minimum) radius of curvature of the apex of the tip, β is a numerical factor, typically[45] around $\frac{1}{5}$, and $r^2\Omega$ is the emitting area. Use of the Fowler-Nordheim equation has shown[45] that Ω should be

[45] E. E. Martin, H. W. Pitman, and F. M. Charbonnier, Wright Air Development Center, Air Research and Development Command, United States Air Force, Wright-Patterson Air Force Base, Ohio.

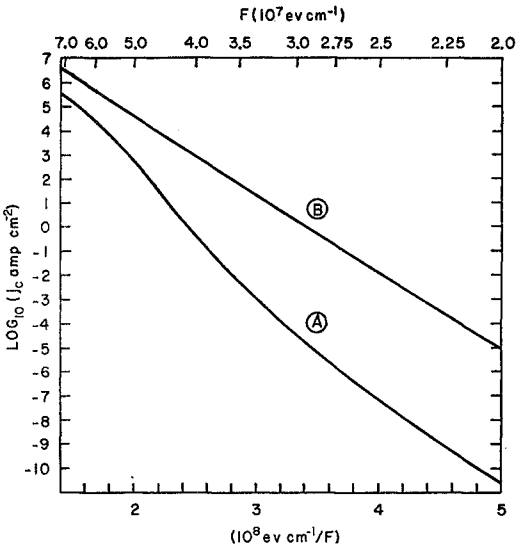

FIG. 7. Field emission from the conduction band (curve A), assuming the surface states model proposed, for n-type germanium at room temperature, by Handler,[38] and from the valence band (curve B).

in the range of about 1 to 4 for representative tip shapes. Substituting numerical values into Eq. (92) leads to $r=2.6\times10^{-5}$ cm and $\Omega=8.3$ with $\beta=\frac{1}{5}$. Due to the uncertain value of β, the experimental results cannot be considered as inconsistent with emission from the valence band simply because Ω is greater than 4.

Allen's experimental results, Eq. (90), can also be compared with the conduction band field emission curve (12,1) in Fig. 6 for which $c=1.1\times10^{10}$ amp cm^{-2} and $w=6.3\times10^8$ ev-cm^{-1}. Thus, using Eq. (92) and Allen's experimental values for C and W, $r=2.9\times10^{-5}$ cm and $\Omega=3.3$ which makes conduction band emission slightly more plausible than valence band emission. However, Allen's data are definitely inconsistent with the straight-line portions of any of the other curves in Fig. 6. The determination of the temperature dependence, if any, of the emission current would have been of interest since field emission from the conduction band depends on the temperature [unless the surface is extremely degenerate and Eq. (82) applies] while field emission from the valence band does not.

Klimin, Sedykh, and Sokol'skaya[22] also measured I as a function of V for Ge and gave results at several temperatures from 295°K to 630°K. They reported that they were unable to obtain the characteristic emission patterns and that their emitters were probably covered by an oxide layer. (Our calculation is thus not really applicable since the surface states distribution is more complex and tunneling through the oxide layer should be considered unless it is very thin.) At 295°K, their experimental results obey Eq. (90) with $C=0.23$ amp and $W=3.8\times10^4$ v. Comparing this with emission from the valence band gives $r=1.0\times10^{-5}$ cm and $\Omega=0.037$. Alternatively, comparing with the conduction band field emission curve (12,1) in Fig. 6 gives $r=1.2\times10^{-5}$ cm and $\Omega=0.15$. Both values of Ω are too low, which sug-

gests a decrease in tunneling probability arising from the oxide layer; however, conduction band emission is again somewhat more likely. This is consistent with the experimental finding that I, at a given V, increases as the temperature rises. It is of interest that at the highest value of V employed, namely 4×10^3 v, J became independent of T. This suggests strong field penetration, leading to an extremely degenerate surface electron distribution so that the temperature-independent Eq. (82), for ζ_s, applies.

Elinson and Vasil'ev's[21] room temperature data (cf. their Fig. 2) also fits Eq. (90) (with $C=0.66$ amp and $W=6.0\times10^4$ v) over a portion of the applied voltage range. The absence of a symmetrical emission pattern again indicated that an oxide layer covered the emitter surface. An attempt to fit the data to either valence band emission or the conduction band emission curve (12,1) gives r values of 1.6×10^{-5} cm and 1.9×10^{-5} cm, and Ω values of 0.043 and 0.17, respectively. These results are close to those deduced from the measurements of Klimin, Sedykh, and Sokol'skaya.[22] Elinson and Vasil'ev also measured the field emission current at 1023°K and obtained a curve which was convex towards the origin on a $\ln J$ against $1/V$ plot. They concluded that this was in qualitative agreement with T-F emission from the conduction band. If their data are replotted as $\ln J$ versus V^2, a straight line is found for V greater than about 4.6×10^3 v. However, comparing this with Eq. (54), it turns out that the deduced range of F values would be too small for T-F emission, i.e., inequality (65) is not obeyed. This is not intended as a stringent test of whether T-F emission applies since it neglects the field dependence of other factors in Eq. (54), but it indicates that a more quantitative analysis is needed to identify the nature of a measured emission current.

Elinson[29] has pointed out that, for sufficiently high emission currents, the hot-electron[46] and Poole-Frenkel[47] effects become important. He calculated the electron temperature $T_e(F_b)$ and the increased free electron density $n_b'(F_b)$, for a partially ionized semiconductor, in terms of the "internal electric field F_b''. Since the calculation is carried out as though F_b were a constant field, acting across a uniform semiconductor, Elinson presumably neglects the presence of a surface space charge barrier, arising from field penetration. The expressions for $n_b'(F_b)$ and $T_e(F_b)$ are inserted into Eq. (36′) for j_{c0} which is then equated with the expression $qn_b'F_b\mu$ where μ is the electron mobility, assumed to be independent of F_b. (This is an unnecessary restriction since the dependence of μ on $T_b(F_b)$ is known for the simple scattering mechanisms considered by Elinson). Thus F_b can be determined and j_{c0} derived as an explicit function of the applied field F.

Elinson's calculation for $n_b'(F_b)$ and $T(F_b)$ really refers to the ohmic bulk region, outside the surface space-charge region. Thus the variation of these quantities, across the surface space region, must be derived before the field emission current can be determined by one of the appropriate results from Secs. 3 or 4. It is for example quite possible that the hot electron and Poole-Frenkel effects are important in the bulk region but may be neglected near the surface, if it is strongly degenerate. Elinson maintained that his theory explained the nonlinearity, in the direction of increased currents at the high-voltage ends of the $\log J-(1/V)$ plots, observed for Al_2O_3,[14] SiO_2,[14] and Ge.[21] However, such an explanation is still open to question until the field penetration effect is incorporated into Elinson's theory.

[46] For a recent review on the hot electron effect see S. H. Koenig, J. Phys. Chem. Solids 8, 227 (1959).
[47] Ia. Frenkel, J. Exptl. Theoret. Phys. 8, 1893 (1938).

APPENDIX 1

From the definitions of E_m and E_x it follows that

$$E_m^{-1}(E_\perp)-E_\perp\leqslant E_x\leqslant A-E_\perp,$$
$$0\leqslant E_\perp\leqslant E_m(A),$$

where $E_m^{-1}(x)$ is the inverse of the function $E_m(x)$ and we have replaced the upper limit on E by A which will ultimately be taken as infinity. Since the Wronskian of the transformation is unity,

$$\int_0^A dE\int_0^{E_m(E)} dE_\perp\cdots\longrightarrow\int_0^{A-E_m(A)} dE_x \times\int_0^{E_\perp(E_x)} dE_\perp\cdots+\int_{A-E_m(A)}^{A} dE_x\int_0^{A-E_x} dE_\perp\cdots, \quad (A.1)$$

where $E_\perp(E_x)$ is the solution of

$$E_x=E_m^{-1}(E_\perp)-E_\perp. \quad (A.2)$$

Thus, carrying out the integration over E,

$$\begin{aligned} j=&\frac{4\pi mkT}{h^3}\Bigg[\int_0^{A-E_m(A)} dE_x\,D(E_x) \times\ln\left\{\frac{1+\exp[(\zeta-E_x)/kT]}{1+\exp[(\zeta-E_x-E_\perp(E_x))/kT]}\right\} \\ &+\int_{A-E_m(A)}^{A} dE_x\,D(E_x)\ln\left\{\frac{1+\exp[(\zeta-E_x)/kT]}{1+\exp[(\zeta-A)/kT]}\right\} \\ =&\frac{4\pi mkT}{h^3}\Bigg[\int_0^{A} dE_x\,D(E_x)\ln\left\{1+\exp\left(\frac{\zeta-E_x}{kT}\right)\right\} \\ &-\int_0^{A-E_m(A)} dE_x\,D(E_x) \times\ln\left\{1+\exp\left[\frac{(\zeta-E_x-E_\perp(E_x))}{kT}\right]\right\} \\ &-\int_{A-E_m(A)}^{A} dE_x D(E_x)\ln\left\{1+\exp\left[\frac{(\zeta-A)}{kT}\right]\right\}\Bigg]. \end{aligned} \quad (A.3)$$

When A tends to infinity, the third integral tends to zero due to the exponential factor. In the second integral the variable of integration E_x is replaced by

$$\mathcal{E}=E_x+E_1(E_x)=E_m^{-1}[E_1(E_x)];$$

therefore

$$E_x=\mathcal{E}-E_m(\mathcal{E}).$$

The integral is then equal to

$$\int_0^A d\mathcal{E}\left[1-\frac{d\mathcal{E}_m}{d\mathcal{E}}\right]D[\mathcal{E}-\mathcal{E}_m(\mathcal{E})]\times\ln\left[1+\exp\left(\frac{\zeta-\mathcal{E}}{kT}\right)\right]. \quad (A.4)$$

Combining it with the first integral and letting A tend to infinity then leads to Eq. (7) in Sec. 2.

APPENDIX II

The quantity

$$t_m-t_1\equiv t[\psi_i/(\psi-E_m)]-t[\psi_i/(\psi_i-\zeta)]\approx[y^2dt(y)/dy]_{y=\psi i/x}(E_m-\zeta)/\psi_i. \quad (A.5)$$

Now, from Eqs. (50), (52), and (61),

$$E_m-\zeta=\psi-\chi(g^2/t_m^2)-\zeta\approx-\chi(2\delta/t_m), \quad (A.6)$$

from which it follows that δ is negative since E_m is greater than ζ. Also, substituting into (A.5), we have

$$t_m-t_1\approx-[ydt/dy]2\delta/t_m. \quad (A.7)$$

Now both y and $dt(y)/dy$ are considerably less than one while t_m is of order one. Thus t_m-t_1 is very small compared to $-\delta$.

APPENDIX III

Various cases of field emission from semiconductors will now be considered to determine when the assumption of a constant Fermi level is reasonable. It will first be assumed that electron emission occurs only from the conduction band. ($j_v=0$). Let j_n be the current density, n the electron density, μ_n the electron mobility, and ϕ_n the quasi-Fermi level for electrons at a point x in the space charge region. Then

$$j_n=n\mu_n d\phi_n/dx. \quad (A.8)$$

The current density j_n will be less than, or equal to, j_c depending on whether or not there is an appreciable hole current at any point in the space-charge region. The change in ϕ_n, across the space-charge region is given by

$$\Delta\phi_n=\int_{-L}^0(j_n/n\mu_n)dx, \quad (A.9)$$

where L is a suitably defined measure of the space-charge region thickness. The variation of ϕ_n may be neglected if

$$\Delta\phi_n\ll kT \quad \text{or} \quad j_c\ll(kT\mu_n)\Big/\int_{-L}^0 dx/n. \quad (A.10)$$

The integral will be estimated by substituting the value for n, assuming a constant Fermi level, which is reasonable if the inequality is obeyed. Thus[27]

$$-\int_{-L}^0 dx/n=(L_D/n_i)\int_{u_b}^{u_s}[e^{-u}/F_{KN}(u_b,u_s)]du, \quad (A.11)$$

where n_i is the intrinsic electron density, L_D is the Debye length [cf. Eq. (81)] and the function F_{KN} is defined by Eq. (80). For a retarding potential barrier ($-\zeta_s\gg-\zeta_b$ or $u_s\ll u_B$), the integral can be approximated by the expression

$$(L_D/n_i)[e^{-u_s}/F_{KN}(u_b,u_s)]=kT/F_sn_s, \quad (A.12)$$

using Eq. (80) and taking n_s as the value of n at the surface. Substituting into inequality (A.10) for j_c, from Eq. (30′) and for the integral, from Eq. (A.12), gives

$$e^{-b_0}\ll[\mu/(kT/2m\pi)^{\frac{1}{2}}q]F_s. \quad (A.13)$$

For n-type germanium at room temperature the expression in square brackets is about 5×10^{-3} ev^{-1} cm, F_s is typically of order 10^3 ev/cm or greater and b_0 exceeds 10 for the examples considered in Sec. 8. Thus the inequality is extremely well satisfied.

There will be a Fermi level variation outside the space-charge region arising from the current flow across the Ohmic (spreading) resistance region in the bulk. This is however accompanied by an equal potential variation and does not lead to any change in carrier density. The separation between the bulk region and space-charge region is of course somewhat arbitrary. In particular, when the barrier height becomes very small, i.e., u_s tends u_b, the integral in Eq. (A.11) may be taken to be L/n_b where n_b is the bulk density of electrons and L is of the order of a Debye length. Thus inequality (A.10) becomes

$$j_c\ll kT\mu_n n_b/L, \quad (A.14)$$

or, substituting for j_c from Eq. (36′),

$$e^{-b_0}\ll[\mu/(kT/2\pi m)^{\frac{1}{2}}q][kT/L], \quad (A.15)$$

which, similarly to Eq. (A.13), is well satisfied.

When the surface distribution of electrons is degenerate, due to field penetration, the Fermi level variation, across that part of the space-charge region which is degenerate, should be negligible, due to its high conductivity. The Fermi level variation, across that part of the space-charge region which is nondegenerate, will also be negligible if inequality (A.14) is satisfied where L is again of the order of a Debye length. For example, if j_c is as much as 10^3 amp-cm^{-2} (the highest value considered in Fig. 6), inequality (A.14) will be satisfied if n_b exceeds 10^{15} cm^{-3}, for room temperature germanium.

By drawing quasi-Fermi level diagrams, for the space charge region, it can be shown that the total variation of the quasi-Fermi level for holes ϕ_p is less than that for electrons in the present case ($j_v=0$ and n-type bulk

material). Hence, it too can be neglected. [There will actually be an electron-hole generation region, just inside the surface, with $(\phi_p-\phi_n)$ positive, followed by a recombination region, with $(\phi_p-\phi_n)$ negative.]

For p-type bulk material (still assuming $j_v=0$), the quasi-Fermi level variations, at least for electrons, will not be negligible when $u_s \gtrsim u_b$) and the methods used in Sec. 7 will not apply. Here, there must be an electron-hole generation region, the electrons diffusing towards the surface and then being emitted while the holes diffuse away from the surface, towards the bulk region. For a sufficiently high value of j_c, the carrier generation may have to be enhanced by avalanche carrier multiplication.

Next, the case of predominant electron emission from the valence band will be considered. Here, there will be a recombination region near the surface. For p-type bulk material only, this is followed by a generation region. The expression for j_v will only be affected by the Fermi energy for the hole distribution at the surface if it is degenerate. The only situation where this is likely to occur is for an initially degenerate p-type surface with a sufficiently high density of surface states to prevent appreciable field penetration. If this is associated with a p-type bulk region, $\Delta\phi_p$ should be negligible as was $\Delta\phi_n$ for the case of predominant conduction band emission from n-type material.

For those cases where the separation between the electron and hole Fermi levels at the surface is negligible (i.e., no net generation or recombination), they will also coincide with the Fermi level for surface states, provided there is no appreciable field emission from the surface states.

The probability that an electron in a surface state, incident on the surface barrier, be emitted is approximately given by Eq. (1) with ψ suitably defined. However, to compare the probabilities, per unit time, for field emission and emission into the conduction or valence bands, requires some knowledge of the surface-state wave functions.

PHYSICAL REVIEW VOLUME 125, NUMBER 1 JANUARY 1, 1962

Magnetic, Thermal, and Optical Properties of the F Center in NaH†*

W. L. WILLIAMS‡
Department of Physics, Dartmouth College, Hanover, New Hampshire
(Received August 11, 1961)

Thermal and optical bleaching and microwave saturation effects on the isotropic resolved electron paramagnetic resonance hyperfine structure of the F center in NaH have been studied. The results indicate that the thermal bleaching is a monomolecular process with an associated activation energy $\epsilon_F=0.38$ ev. A model similar to the print-out effect in silver halides is proposed for the bleaching mechanism. The wavelength of maximum optical absorption is 3.22 ev. The value of the characteristic spin relaxation time $(T_1T_2)^{\frac{1}{2}}$ is 1.7×10^{-5} second. The g value for the F-center electron is 2.0025 ± 0.0003.

I. INTRODUCTION

THE resolved isotropic hyperfine structure of the electron paramagnetic resonance absorption of F centers in NaH was recently observed.[1] This paper reports the results of further measurements of the properties of this F center. Section II describes the experimental details. The results of thermal bleaching measurements, discussed in Sec. III, indicate that the F-center destruction is a monomolecular process. The thermal activation energy for this process is determined and a model involving the growth of colloidal sodium is proposed which is similar to the print-out effect in silver halides. Section IV is a description of the optical bleaching measurements which give a value for λ_0, the wavelength of maximum optical absorption. An order of magnitude result for the characteristic spin relaxation time $(T_1T_2)^{\frac{1}{2}}$, obtained from saturation measurements, is given in Sec. V. The F-electron g value, determined using the Breit-Rabi equation to second order, is given in Section VI. Section VII is a brief summary of the results.

II. EXPERIMENTAL

All the measurements described here were made using a conventional superheterodyne paramagnetic resonance spectrometer employing phase-sensitive detection. The microwave frequency is approximately 9.1 kMc/sec. The sample cavity is rectangular and operates in the TE_{101} mode. The dc magnetic field is modulated at 560 cps. The microwave frequency was measured with a cavity wavemeter calibrated against WWV using a frequency multiplier. The magnetic field

† Research supported by a grant from the National Science Foundation.
* This work is based upon a thesis submitted by the author to the Department of Physics, Dartmouth College, in partial fulfillment of the requirements for the M.A. degree.
‡ Present address: Josiah Willard Gibbs Research Laboratories, Yale University, New Haven, Connecticut.
[1] W. T. Doyle and W. L. Williams, Phys. Rev. Letters 6, 537 (1961).